ANSTO/C615

A REPORT TO THE

REPOSITORY TECHNICAL ASSESSMENT GROUP
BUREAU OF RURAL SCIENCES

on

TECHNICAL STUDIES FOR SITE SELECTION OF A NATIONAL LOW-LEVEL RADIOACTIVE WASTE REPOSITORY

VADOSE ZONE HYDROLOGY AND RADIONUCLIDE RETENTION

ASSESSMENT OF DRILL SAMPLES TO ASSIST SELECTION OF FIVE PREFERRED SITES

ANSTO Environment Division

CSIRO Land and Water

January 2000

ANSTO/C615

A REPORT TO THE

REPOSITORY TECHNICAL ASSESSMENT GROUP
BUREAU OF RURAL SCIENCES

on

TECHNICAL STUDIES FOR SITE SELECTION OF A NATIONAL LOW-LEVEL RADIOACTIVE WASTE REPOSITORY

VADOSE ZONE HYDROLOGY AND RADIONUCLIDE RETENTION

ASSESSMENT OF DRILL SAMPLES TO ASSIST SELECTION OF FIVE PREFERRED SITES

A Collaborative ANSTO/CSIRO Technical Study

by

John R. Harries and Timothy E. Payne
Australian Nuclear Science and Technology Organisation
and
David Smiles
CSIRO Land and Water

January 2000

EXECUTIVE SUMMARY

Twenty-six samples of material obtained from the Phase 1 drilling program to select a site for a National Low Level Radioactive Waste Repository were selected as representative of materials found in 12 bore holes.

X-ray diffraction measurements and batch adsorption Cs-137 experiments were performed on all samples. Hydrodynamic dispersion/reaction experiments measured retardation of the nuclides tritium, cesium and cobalt on three of these samples. These latter experiments involved absorption of solution into relatively dry soil and approximated conditions that might arise during an inadvertent leak of contaminated water into the regolith.

The results of these experiments were compared with each other and with field and bore log data obtained during the drilling program.

It was demonstrated that

i) field texture descriptions are roughly consistent with XRD data but must be interpreted with caution in predicting radionuclide retardation;

ii) clay mineralogy, as measured by XRD, is a good indicator of radionuclide retention properties;

iii) adsorption of cesium is strongly related to clay mineralogy. Layers of mica, illite and smectite rich materials between the repository and the water table would be beneficial for cesium retardation;

iv) the minerals of greatest relevance for cesium sorption are mica/illite and smectite. Smectite in the surface soil is the strongest absorber of 1 mmol/L cesium, whereas illites and degraded micas are the strongest absorbers of trace cesium;

v) column experiments can be used to measure radionuclide retardation under conditions which are representative of field saturation and geochemistry; and

vi) tritium moves as does water and suffers no retardation.

These experiments indicate the importance of quantitative and unambiguous estimates of the hydraulic and adsorptive properties of the regolith materials at the possible sites for the repository. Hydraulic properties need to be measured on samples that represent field conditions. Adsorption estimates can be based on batch experiments, but require confirmation using column experiments to ensure that they are applicable to the unsaturated conditions representative of the regolith at the sites being considered for the repository.

The report concludes with a recommended set of measurements and surface descriptions that would provide a sound basis for assessing any site in terms of vadose zone hydrology and radionuclide retardation.

Table of Contents

EXECUTIVE SUMMARY 3
1. INTRODUCTION 5
2. SAMPLE SELECTION FOR STUDIES 6
3. X-RAY DIFFRACTION 6
4. BATCH MEASUREMENTS 7
   4.1 Method 7
   4.2 Results of Batch Experiments with Trace Cesium 8
   4.3. Results of Batch Experiments with 1 mmol/L Cesium 9
5. COLUMN MEASUREMENTS 9
   5.1 Method 9
   5.2 Results of Column Experiments 10
   5.3 Discussion of Column Experiment Results 12
6. CONCLUSIONS AND RECOMMENDATIONS 12
7. ACKNOWLEDGMENTS 13
8. REFERENCES 13

1. INTRODUCTION

The selection of the site for Australia's National Low-Level Radioactive Waste Repository will be based on criteria recommended in the "Code of Practice for the Near-Surface Disposal of Radioactive Waste in Australia 1992" issued by the National Health and Medical Research Council (BRS 1997). Criteria C and G for site selection are:

Criterion C: The geological structure and hydrogeological conditions should permit modelling of groundwater gradients and movement, and enable prediction of radionuclide migration times and patterns.

Criterion G: The site should have suitable geochemical and geotechnical properties to inhibit migration of radionuclides and to facilitate repository operations.

These criteria relate to movement and fate of radionuclides that might be released inadvertently from the repository to the regolith. Movement of nuclides depends on the rate of water movement and their retardation which results from chemical reaction with, and adsorption on, the regolith material. Kellett *et al.* (1999) have described the regional groundwater properties.

Preliminary desk-top studies by ANSTO and CSIRO (Harries *et al.*, 1998) identified key desirable vadose zone features of sites in central northern South Australia where a repository might be sited. A supplementary study by ANSTO and CSIRO (Harries *et al.*, 1999) confirmed that water balance calculations based on measured profile properties and 30 years of historical daily rainfall and evaporation data accorded well with measured soil water profiles. The estimates of ground water recharge for these sites and estimates of nuclide movement, based on this approach, are expected to be relatively reliable. The sites examined in these exploratory studies were generally representative of soils of the area but were not close to any of the potential sites under consideration.

This report presents the results of measurements on representative samples from the Phase 1 drilling program in the central north region of South Australia. Measurements include:

i) X-ray diffraction [XRD] measurements that provide the relative abundance of key clay minerals which largely control the adsorption and retardation of chemical species in the profile. These data are compared with aspects of the field descriptions of texture;

ii) batch measurements of adsorption (distribution coefficients) of radionuclides that might be released inadvertently in materials characteristic of the repository; and

iii) hydrodynamic dispersion experiments using tritium, cesium-137 and cobalt-60 to determine whether adsorption data measured in the batch experiments can be used to predict nuclide retardation during unsteady unsaturated soil water movement in conditions approximating the field.

Finally, a measurement protocol for characterisation of selected sites is proposed.

2. SAMPLE SELECTION FOR STUDIES

The Phase 1 Drilling Program obtained regolith profiles at 11 sites in the mid-north of South Australia. Drill samples were collected by cyclone for each one metre interval of the drill travel. The reverse circulation technique means these samples are relatively clean and not contaminated by material from above the indicated depth. The air hammer drilling process, however, results in substantial physical modification of the material.

The drilling program provided information on the depth to the water table and rate of drilling which is indicative of the strength of local material and hardness of rock. Jim Kellett (BRS) also determined a "texture" expressed in pedological terms based on manipulation of drilled material and on visual inspection under a binocular microscope. Because drilling is structurally destructive, this texture estimation does not simply relate to the field texture of the regolith column. Surface soil profiles were not described and profile mineralogy is also lacking.

For the present study, drill samples representative of the geologies/lithologies at the sites were selected on the basis of inspection of washed samples from each metre of depth prepared by Jim Kellett (BRS) during drilling and an assessment of the drill logs. The aim was to select a limited number of samples that were representative of the conditions expected at the 11 drill holes. The selected samples are listed in Table 1 together with a short summary description of the samples.

3. X-RAY DIFFRACTION

The presence of clay minerals is advantageous for radionuclide retention, although different radionuclides show affinities for particular mineral surfaces. X-ray Diffraction (XRD) measurements were used to determine which clay minerals were present in the 26 samples. Data derived from these exploratory XRD measurements are presented in Table 2, where the following designations are used:

D – dominant [>60%]

CD – co-dominant where several peaks were equally dominant

SD – sub-dominant [20-60%]

M – minor [5-20%] and

T – trace [<5%]

The XRD identification of the clay minerals kaolinite and smectite is unambiguous. The presence of these minerals is associated with weathered sediments and soils; they are not associated with igneous lithology and are unlikely in metamorphosed material. We expect these clay minerals to have cationic retardation associated with surface adsorption, particularly the smectite.

XRD identification of the clay mineral illite is ambiguous because the XRD signal can be confused with mica. These materials differ in their adsorptive capacity. Illite has a net negative surface charge of about 40 mmols of charge /100 grams of clay and will be intermediate between kaolinite and smectite in its ability to adsorb (and retard) cationic nuclides. Mica has a very low surface charge and its adsorption and retardation ability is in general small, although it is reported to have a high selectivity for trace amounts of cesium (Cornell 1993).

Smectite appears to be confined to the near surface (1-3 m) across sites examined in this exploratory study. Kaolinite is found well below the soil surface. Eight materials were identified by XRD as having clay mineral suites likely to be associated with strong cationic nuclide retardation, for example have an M or greater for kaolinite or smectite.

The XRD data offer only a qualitative indication of the relative amount of key minerals. A particle size analysis on less disturbed samples is needed for a quantitative interpretation.

4. BATCH MEASUREMENTS

The ability of the geologic materials between the base of the repository and the water table to adsorb nuclides and retard their transfer relative to water movement is a key issue for siting the repository. Batch experiments compare the different geologic materials in terms of their ability to adsorb cesium-137. The results provide an indication of the *relative* ability of these materials to retard any cesium-137 released from a repository.

The batch technique used here measures adsorption of cesium from a standard solution at a low solid/liquid ratio. This is dissimilar to field conditions in the unsaturated zone of the arid environment where the solid/liquid ratio is high, but the measurement is rapid, reproducible and relatively inexpensive. The column experiments described in Section 5 use solid/liquid ratios comparable to field conditions.

Radionuclide adsorption on mineral surfaces is expressed as a distribution coefficient (K_d) using the equation:

$$K_d = \frac{C_i - C_f}{C_f} \bullet \frac{V}{m} \quad \text{mL g}^{-1}$$

where C_i and C_f are the initial and final amounts of radionuclide in the aqueous phase (Bq/L), V is the volume (30 mL) and m is the mass of soil (0.3 g or 3 g). The distribution coefficient (K_d) is commonly used as a means of assessing the mobility of radionuclides in the environment and for comparing adsorption data obtained from different sources (McKinley and Scholtis 1992; Sheppard and Thibault 1990).

4.1 Method

The sorption experiments described in this section were undertaken with a background electrolyte of 0.5 mol/L NaCl and a solid/liquid ratio of 1:100. The 0.5 mol/L NaCl was selected to be similar to the composition of soil water likely to participate in transport of radionuclides. The samples were sieved at 1 mm to remove larger fragments and then dried at 40–50^{o}C prior to adsorption experiments.

Two series of experiments were undertaken

i) with a trace amount of cesium

ii) with higher (1 mmol/L) total cesium. These experiments were carried out after the addition of non-radioactive cesium as CsCl.

The aim of using these different conditions was to investigate the chemical and mineralogical controls on sorption. The experimental conditions are not necessarily similar to those expected near a repository, particularly in experiments with the higher amount of cesium.

The experimental duration was three days. In the first 24 hours, the cesium-137 was not present and the solids were pre-equilibrated with the background electrolyte. The pH was measured at the end of this initial period. The radionuclide, which is supplied in an acid solution, was then added, and the system was immediately returned to its equilibrium pH value. The samples were gently shaken in unsealed centrifuge tubes at room temperature. After 48 hours contact time, the solid and liquid phases were separated by centrifugation and the cesium-137 content of the clear supernate was measured by γ-spectrometry.

K_d values on the selected materials were calculated using the equation above and are given in Table 3.

4.2 Results of Batch Experiments with Trace Cesium

Based on the K_d values in Table 3, the migration of trace cesium in these materials would be expected to be greatly retarded relative to water movement. For K_d >200 mL/g, cesium would be retarded by approximately 3 orders of magnitude compared to water flow.

It is apparent from the order of increasing K_d values (Table 3) that the field geological description is a useful indicator of the likely sorptive properties of the materials. The adsorption data for trace cesium suggest that materials described as shale or siltstone tend to have higher values of K_d and hence will tend to retard movement of cesium more than sandstone or quartzite. For example, 6 of the 7 samples exhibiting the weakest adsorption of trace Cs (K_d below 500 mL/g) are described as either quartzite or sandstone whilst the samples with high adsorption of Cs (K_d above 1000 mL/g) are mostly comprised of materials containing fine-grained sediments such as siltstone or shale. However, there are some anomalies between the field descriptions and the K_d values for trace cesium. For example, the two materials described as micaceous sandstone (boreholes 40 (45-46 m) and 41 (31-32 m)) yielded very different K_d values of 1590 mL/g and 386 mL/g respectively. This may be due to a different degree of weathering. The XRD examination revealed that these samples have different mineralogies, and in this instance the field description is not a good predictor of the sorption properties.

Table 3 also compares the K_d values for trace cesium with the presence of smectite, mica/illite and kaolinite. The high K_d values for trace cesium tend to be associated with samples having a significant abundance of mica / illite as determined by XRD. The materials containing greater than 20% illite/mica have high K_d values (>1200 mL/g). The 12 materials in which mica/illite are present in minor (>5%) or sub-dominant (>20%) amounts have K_d values for trace Cs that exceed 650 mL/g. The other materials that contain trace or undetectable mica/illite have K_d less than 650 mL/g. These results demonstrate a strong correlation between the presence of mica/illite and the sorption of trace cesium.

This correlation between the abundance of mica/illite and trace cesium sorption is in good agreement with the cesium adsorption data reviewed by Cornell (1993). In a survey of all cesium sorption data for *pure* minerals, mica showed a high selectivity for trace cesium. This was attributed to the high layer charge density and the presence of highly selective sorption sites (frayed edge sites). Similarly, Cornell reported that illites contain some interlayer edge sites, which are highly selective for cesium uptake. Cornell (1993) also reported that although montmorillonite possesses a large number of interlayer sites, these are not very selective for cesium. Thus, mica and illite play the major role at the low cesium concentrations of these experiments with trace cesium. The results in Table 3 show that the presence of smectite, e.g. in samples 16 (2-3 m), 16 (1-2 m) and 12 (1-2 m), does not result in an increased sorption ability for trace cesium.

4.3. Results of Batch Experiments with 1 mmol/L Cesium

The sorption data obtained in experiments with 1 mmol/L cesium are given in Table 3. For 1 mmol/L total cesium, the efficiency of adsorption is reduced and smectite appears to be the most important clay mineral. The increase of total cesium by several orders of magnitude reduced the K_d values and changed the ranking of some samples.

As with the sorption data for trace cesium, the field geological description gives a general indication of the trend in K_d values. Materials such as siltstones and surface clay materials tend to perform better than sandstones and quartzite. The samples containing significant amounts of smectite clearly have a higher capacity for 1 mmol/L cesium, but in this case the mica/illite content as measured by XRD is not such a good indicator of the K_d. Three of the four highest K_d values are for materials containing over 20% smectite. These materials did not perform so well at trace levels of cesium (Table 3). The higher K_d values for the smectite-rich materials at the higher cesium concentration are in accordance with the review of Cornell (1993), who observed that montmorillonites adsorb more total cesium than illites, although the latter materials are stronger adsorbers for trace cesium.

The batch experiments demonstrate that the minerals of greatest relevance for cesium sorption are mica/illite and smectite. The highly selective sorption sites on mica and illite are important for trace cesium, whereas the high total site availability of smectite is significant when the total cesium is higher (1 mmol/L). Layers of mica, illite and smectite rich materials between the repository and the water table would be beneficial for cesium retardation.

5. COLUMN MEASUREMENTS

The selection of the three materials for hydrodynamic dispersion measurements in columns of material was based on drill log and the qualitative XRD results, with the intent to include the main mineralogical types. The samples selected for the hydrodynamic measurement were:

i)	A sample containing gypsum and smectite	Sample #16:1-2m
ii)	A sample containing subdominant kaolinite	Sample #16:10-11m
iii)	A sample containing kaolinite and mica/illite	Sample #14:19-20m

5.1 Method

The column experiments were conducted with material that passed a 2-mm sieve. Initial tests on the samples containing smectite [Sample #16:1-2m], and kaolinite [Sample #16:10-11m] were conducted using water and saturated $CaSO_4$ solutions to "bed" the method in and establish behavioural limits on the materials. The $CaSO_4$ was found to be necessary to maintain the structural stability of these materials. All experiments involving nuclide traces in solutions are therefore based on saturated $CaSO_4$ (≈30 millimoles of charge /L).

Some swelling occurred in the experiments, which makes a physical space coordinate system unreliable. The experiments were analysed in terms of both physical space and material coordinates based on the distribution of the solid component of the soil. A water-based coordinate system is used to compare mobility of nuclides. The use of these coordinate systems gets over the swelling problem and also reduces the effects of inevitable slightly different column packing.

The experimental methods, based on sectioned columns of unsaturated but uniformly moist fine soil, and the theoretical analysis, are described by Smiles *et al*. (1981) and Bond *et al.* (1982). A saturated $CaSO_4$ solution containing the nuclides

i) H-3 as tritiated water at a concentration of 479 Bq/mL

ii) Cs-137 at a concentration of 249 Bq/ml, and

iii) Co-60 at a concentration of 218 Bq/ml

was applied to the end of each column at zero water potential. The advance of the wetting front was observed and, at two different elapsed times, experiments were terminated to measure the spatial distributions of water and solute.

5.2 Results of Column Experiments

Figures 1 (a-c) show the gravimetric water contents, expressed as a function of the solid material distance divided by the square root of the time at which the profile was observed. The solid material distance is the cumulative mass of solid per unit area measured away from the inflow surface. Its use eliminates the need to consider volume change and, to some extent, structural instability associated with swelling (Smiles 1997). Scaling in terms of distance divided by the square root of time for experiments terminated at substantially different times indicates that basic initial and boundary conditions on the experiments are realised and that diffusion equation theory can be applied to extend the experimental data in both distance and time.

These water content profiles scale reasonably bearing in mind that they are exploratory experiments. The variability within sets, which is most evident in Sample 14:19-20m, results from some unevenness of packing, from swelling and perhaps structural instability because relatively low concentration solution displaces soil solution of initially high soluble salt concentration (as is evident below). The variability is not great enough to obscure critical differences between the materials. We may compare these profiles on the basis of

i) The infiltration sorptivities of these materials. The sorptivity identifies the cumulative amount of water the sample absorbs in unit [square root of] time

ii) The advance of the wetting front, which indicates the distance the water will move under comparable water potential conditions.

Comparison of the advance of the wetting fronts is more revealing in this study. Inspection of the three figures, 1 (a-c), shows that the three samples rank in the proportions:

$$\text{Sample \#16:1-2 / Sample \#16:10-11 / Sample \#14:19-20} \approx 0.25 / 0.5/1.6$$

Since the transfer of nuclides will, in general, be related to the advance of the wetting front, Sample #16:1-2m is hydrologically more desirable than Sample #16:10-11m (by a factor of 2), and Sample #16:10-11m is, in turn, about three times more effective that Sample #14:19-20m in limiting water flow.

These observations must be qualified by the experimental conditions. We believe them to be appropriate, however, for these circumstances. This is because in each case, the initial water content approximates that at 15 bars water potential. Previous studies (Harries *et al*., 1999) indicate that this water content will characterise the profiles beyond the root run of the native vegetation, so the initial water content is appropriate. The boundary condition (water potential ≈ 0) is also appropriate because we cannot expect seepage from a trench at water potentials less than zero. Comminution of the solid during drilling remains an inescapable difficulty until undisturbed samples can be obtained, but comparison between samples should be valid.

Interestingly, the infiltration sorptivities of these materials, calculated by integrating under the curves of Figures 1 (a)-(c), show that the sorptivity values for Sample #16:1-2m [≈0.047 $cm.min^{-1/2}$] and Sample #16:10-11m [≈0.048 $cm.min^{-1/2}$] are essentially indistinguishable. This arises because Sample #16:1-2 appears to have a greater clay content than does Sample #16:10-11; which results in significantly different water contents of these samples behind the wetting fronts as shown in the figures.

The ranking based on the advance of the wetting front is objective, since the initial and boundary water potential conditions are well-defined and permit quantitative comparison between the samples for the conditions of the experiments.

Figures 2 (a-c) show the distribution of water soluble salts and of tritiated water in each sample expressed in a solid based space coordinate divided by the square root of time. The concentrations are normalised

i) in the case of tritium relative to the inflow concentration (479 Bq/mL) and

ii) in the case of the water soluble salt by the average distal solution salt concentration. In the case of both Samples #16:1-2m and #16:10-11m this value was 200 mS/cm. In the case of Sample #14:19-20m the value was 100 mS/cm. That is, the soil solution salt concentration of the latter material (in approximate equilibrium with 15 bars water potential) is approximately half that of either Sample #16:1-2m or #16:10-11m (at a similar water potential).

The tritium front, identified with an inflection in the concentration curve, corresponds in each case to an inflection in the receding soil solution salt profile. This is consistent with the notion that the tritium front should correspond with a "piston front" which would exist if the invading solution displaced, in its entirety, the soil water originally present. Displacement of solute front relative to the "piston front" reflects the degree to which the solute is retarded relative to the moving soil water. Coincidence of the tritium front and the piston front is expected of tritiated water, which behaves effectively as water (cf Bond *et al*. 1982). Displacement of a solute front from the piston front is, in principle, predictable using K_d.

The piston front is identified as the origin of a water-based coordinate system in such experiments (Smiles *et al*. 1981). Figures 3 (a-c) show the data of Figures 2 (a-c) presented in this water based coordinate system. Evidently the initial soil solution concentration, represented by data to the right of the piston front, is great relative to that of the invading solution. This substantial decrease in solute concentration at the piston front affects the structural stability of the columns. It appears to give rise to the variability in the water content profiles. The use of the water based coordinate (shown in Figures 3 (a-c)), appears to eliminate the effects of structure change evident in Figures 2 (a-c), particularly in the case of Sample #14:19-20. The evidence for this is the relatively good scaling in terms of material (water) distance divided by the square root of time, with the solute front for experiments terminated at different times, coinciding with the piston front (identified as the coordinate origin), for each material.

Figures 4 (a-c) show the distribution of the nuclides Cs-137 and Co-60 in each sample expressed in terms of the solid based space coordinate. These cationic nuclides, as expected in the materials containing smectite and kaolinite, are retarded to the extent that in Samples #16:1-2m and #16:10-11m the nuclide did not escape the first section of the column. In Sample #14:19-20m material, however, a significant amount of Co-60 travelled beyond the first column section. The divalent Co^{2+} advanced further than the monovalent Cs^{+}. From the point of view of cobalt retardation, sample #16:1-2 and #16:10-11 materials are more desirable than the Sample #14:19-20 material.

5.3 Discussion of Column Experiment Results

The column experiments show that the materials represented by Samples #16:1-2 and #16:10-11 are more desirable than the material represented by Sample #14:19-20 both from the point of view of radionuclide retardation and from considerations based on the hydraulic properties of repacked drilled samples.

The relative ranking of the retardation in the three samples is consistent with the ranking of the distribution coefficients measured in the batch experiments for the 1 mmol/L total cesium (shown in Table 3). The adsorption data suggest that materials described as siltstones and shales, some of which contain kaolin or smectite, are relatively retentive of cesium and cobalt, so the occurrence of these materials from a depth of 15m to the water table is desirable for repository siting.

Movement of tritium as tritiated water is indistinguishable from that of water as we might expect. Significant transfer of tritium in the vapour phase in these soils is unlikely. This is because the partition coefficient between tritiated water in the liquid and the vapour phase is of order 10^5. As a result, while the *velocity* of tritiated water in the vapour phase is relatively great compared with that in the liquid; the *flux* [=*velocity ´ concentration*] remains tiny till the volume fraction of liquid water is less than a few percent (Smiles *et al*. 1993a, b; Smiles *et al*. 1995). Data presented by Harries *et al*. (1999) show that the volume fraction in these profiles will approximate the wilting point water contents [>0.15] so vapour transfer can be neglected.

6. CONCLUSIONS AND RECOMMENDATIONS

Measurements of radionuclide adsorption in batch experiments, and measurements of nuclide retardation during absorption of water by columns of relatively dry soils, have been undertaken on representative samples from the Phase 1 drilling program. The samples were from reverse circulation drilling, and there is uncertainty on the effect of the physical modification of the samples in the drilling process. The properties of the present samples collected by reverse circulation drilling need to be compared with the properties of samples collected by diamond core drilling.

The results presented in this report are internally consistent and indicate the relative retardation between different mineralogies. A reasonable correlation was found between adsorption and XRD results. The results show that the adsorption, and hence the retardation, is related to the specific clay minerals occurring in the profile as determined by XRD. Smectite-rich surface soils are the strongest adsorbers of 1 mmol/L cesium, whereas as illites and degraded micas are the strongest adsorbers of trace cesium.

The following measurements are necessary to provide an objective basis for assessing sites under Criteria C and G.

i) Surface soil [0-2m] profile descriptions sufficient to undertake water balance modelling. These are necessary to ensure that water balance estimations for these preferred soils are reliable (cf Harries *et al*., 1999). The surface soil, relief and vegetation which control the water balance and hence the deep drainage that will effect nuclide movement throughout the regolith must be described.

ii) Estimates of hydraulic properties of the regolith are required to infer flux rates, flow velocities and residence times for water moving from the surface to the

water table. The residence time is the depth to the water table divided by the pore water velocity. Long residence times are desirable for any nuclides inadvertently released from the repository to travel to the water table. Water balance estimations based on historical rainfall and evaporation data are required determine the "deep drainage" at the site. This estimation, together with depth to the water table also permits calculation of the "residence time" of the pore water.

iii) Clay mineralogy and particle size distribution measurements are required to provide estimates of retardation of nuclides relative to the deep drainage water in the context of the residence time for the pore water above the water table. It is suggested that XRD measurement be performed on all cores and horizons where the bore log indicates mineralogical change. These data provide a basis for quantitative ranking of sites at least in relation to clay mineralogy.

iv) Radionuclide adsorption measurements on representative samples to determine the retardation of nuclides in the profile. These measurements should be performed on key horizons and materials and should include both batch and column experiments as described in this report. Nuclide adsorption properties of characteristic soils and regolith are used to predict the way various important nuclides will move with and be retarded relative to unsaturated water flow in the soil and to deep drainage.

7. ACKNOWLEDGMENTS

The authors gratefully acknowledge the assistance of Gordon McOrist (ANSTO) with radiochemical analysis and Takashi Itakura (ANSTO) with the batch adsorption experiments.

8. REFERENCES

Bond, W. J., Gardiner, B. N. and Smiles, D. E. 1982. Constant Flux Absorption of a Tritiated Calcium Chloride Solution by a Clay Soil. *Soil Science Society of America Journal* **46**, 1133-1137.

BRS 1997. A Radioactive Waste Repository for Australia: Site Selection Study — Phase 3: Regional Assessment: A Public Discussion Paper. Bureau of Resource Sciences, Canberra.

Cornell, R.M. 1993. Adsorption of Cesium on Minerals: A Review. *Journal of Radioanalytical and Nuclear Chemistry*, **171**, 483- 500.

Harries, J. R., Kirby, J. M., Payne, T. E. and Smiles, D. E. 1998. Technical Studies for Site Selection of a National Low-level Radioactive Waste Repository. Vadose Zone Hydrology and Radionuclide Retardation. A report to the Department of Primary Industries and Energy, Bureau of Resources Science. ANSTO/C-563.

Harries J. R., Payne T. E, Green T. W., Kirby J. M. and Smiles D. E. 1999. Technical Studies for Site Selection of a National Low-level Radioactive Waste Repository: Vadose Zone Hydrology and Radionuclide Retention - Supplementary Study - A Report to the

Department of Industry Science and Resources, Bureau of Resource Science ANSTO/C-575

Kellett, J., Veitch, S., McNaught, I., and van der Voort, A. 1999. Hydrogeological Assessment of a Region in central northern South Australia. Division of Land and Water Sciences. Bureau of Rural Sciences, Australia

McKinley, I. G. and Scholtis, A. 1992. Compilation and Comparison of Radionuclide Sorption Databases used in Recent Performance Assessments. Proceedings of a NEA Workshop on Radionuclides from the Safety Evaluation Perspective, 16-18 October 1991, Interlaken Switzerland, OECD.

Sheppard, M. I and Thibault, D. H. 1990. Default Soil Solid/Liquid Partition Coefficients, Kds, for Major Soil Types: a Compendium. *Health Physics*, 59, 471-482.

Smiles, D. E. 1997. Water Balance in Swelling Materials: Some Comments. *Australian Journal of Soil Research*, **35,** 1143-52**.**

Smiles, D. E., Gardner, W. R. and Schulz, R. K. 1993a. Three Dimensional Redistribution of Tritium from a Point of Release into a Uniform Unsaturated Soil: A Deterministic Model for Tritium Migration in an Arid Disposal Site. NUREG/CR-5980, January 1993, US Nuclear Regulatory Commission, Washington DC.

Smiles, D. E., Gardner, W. R., Schulz, R. K., and O'Donnell, E. 1993b. Tritium Migration in Arid Soils. 15th Annual US Department of Energy Low Level Radioactive Waste Management Conference. Phoenix, AZ.

Smiles, D. E., Gardner, W. R. and Schulz, R. K. 1995. Diffusion of Tritium in Arid Disposal Sites. *Water Resources Research* **31:**1483-1488.

Smiles, D. E., Perroux, K. M, Zegelin, S. J. and Raats, P. A. C. 1981. Hydrodynamic Dispersion During Constant-rate Absorption of Water by Soil. *Soil Science Society of America Journal* **45**: 453-458.

Table 1. Selected Representative Drill Samples

#	Borehole	Depth	General Description
1	16	1 to 2 m	Clay
2	12	1 to 2 m	
3	16	2 to 3 m	Silcrete
4	13	7 to 8 m	Banded quartzite and kaolinitic clays
5	16	10 to 11 m	
6	12	9 to 10 m	Yellowish clay bands in quartzite
7	13	10 to 11 m	Grey/green clay
8	13	21 to 22 m	
9	14	13 to 14 m	Green and grey clays
10	14	19 to 20 m	
11	14	23 to 24 m	
12	7	9 to 10 m	Arcoona Quartzite
13	10	23 to 24 m	
14	16	30 to 31 m	
15	14	28 to 29 m	Corraberra Sandstone
16	13	31 to 32 m	
17	14	40 to 41 m	
18	16	46 to 47 m	
19	14	55 to 56 m	Corraberra Sandstone (below water table)
20	16	77 to 78 m	
21	14	32 to 33 m	Siltstone
22	14	33 to 34 m	
23	16	24 to 25 m	Shale with trace sulfides
24	16	37 to 38 m	
25	40	45 to 46m	Highly micaceous (sericitised) sandstones of the Corraberra Sandstone
26	41	31 to 32 m	

Table 2. XRD DATA and FIELD DESCRIPTIONS

Sample	Quartz	Kaolin	Gypsum	Mica/ Illite	Micro-cline	Albite	Palygorskite	Smectite	Calcite	Anatase	Halite	Hematite	Siderite	Goethite	Chlorite	Field "texture" description
7 (9-10m)	D	T	T													Arcoona quartzite
10 (23-24m)	D	T		T	T											Arcoona quartzite
12 (1-2m)	D	T	SD		T		M	M	T	T						Clay
12 (9-10m)	D	T	T	T	T		?T				T					Clay bands in quartzite
13 (7-8m)	D	T	T	T						T	T					Quartzite/kaolinite bands
13 (10-11m)	D	T	T	T	T		?T				T					Gray/green clay*
13 (21-22m)	D	T		T	T											Gray/green clay*
13 (31-32m)	D	T		T	M		?T		T			T	T			Corraberra sandstone
14 (13-14m)	D	M		M	M		?T				T					Gray/green clay
14 (19-20m)	D	M	T	M	M						T					Gray/green clay
14 (23-24m)	D	T		M	M		?T			T	T					Gray/green clay
14 (28-29m)	D	T	T	M	M		?T				T			T		Arcoona quartzite
14 (32-33m)	D	T		SD	SD	M				T		M		M	T	Siltstone
14 (33-34m)	D	T		SD	SD	M				T		M			T	Siltstone
14 (40-41m)	D	T	T	T	M	M	?T					T	T		T	Corraberra sandstone
14 (55-56m)	D			T	M		?T					T			T	Corraberra sandstone

- Approximate composition determined from the strongest line of each component using the following designations: D - dominant (>60%), SD - sub-dominant (20-60%), M – minor (5-20%), T - trace (<5%).
- Palygorskite was not positively identified in any of the samples, however, trace levels may be present.

TABLE 2 [cont]

Sample	Quartz	Kaolin	Gypsum	Mica/ Illite	Micro-cline	Albite	Palygorskite	Smectite	Calcite	Anatase	Halite	Hematite	Siderite	Goethite	Chlorite	Field "texture" description
16 (1-2m)	D	T	SD				M	M	T	T		T				Clay
16 (2-3m)	D		SD					M		T						Silcrete*
16 (10-11m)	D	SD	T	M			?T	T		T	T					Banded quartzite/kaolinite
16 (24-25m)	CD	CD		CD	M	T				T		M			T	Shale with sulphide traces
16 (30-31m)	D	M	T	M	M		?T			T						Arcoona quartzite*
16 (37-38m)	D	T		M	M	T				T		T	M		T	Shale with sulphide traces
16 (46-47m)	D	T		M	M		?T			T		T	M		T	
16 (77-78m)	D			T	M	T			T			T	T		T	Corraberra sandstone
40 (45-46m)	D	T		M	SD	T		T		T		M		T		
41 (31-32m)	D	T		T	M	T		T	T	T		T				
W1	D	M		T	M	T		M	T	T		T				Light clay
W2	CD	T		T	T	T		CD	T	T	T	T				Medium clay

- Approximate composition determined from the strongest line of each component using the following designations: D - dominant (>60%), SD - sub-dominant (20-60%), M – minor (5-20%), T - trace (<5%).
- Palygorskite was not positively identified in any of the samples, however, trace levels may be present.

The table relates these mineralogical data to "texture" descriptions made during drilling.

Cases where the texture description differs from the XRD data are starred (*). In the main correspondence is reasonable.

Table 3. K_d data for Cesium arranged in order of decreasing K_d for trace cesium, showing relationship to XRD results for smectite (S), mica/illite (M/I) and kaolinite (K). A high value of K_d is preferred for the repository site.

Hole	Depth (m)	K_d (mL/g)		Description (based on field log)		XRD		
		Trace Cs	1 mmol/L Cs	Main	Minor	S	M/I	K
14	32-33	1706	5.22	Siltstone: laminated grey silicified fine sandstone and purple siltstone	Trace mica	0	SD	T
40	45-46	1590	10.8	Micaceous sandstone: pale purple brown micaceous silicified fine sandstone		T	M	T
14	33-34	1304	4.69	Siltstone: Maroon siltstone		0	SD	T
14	28-29	1290	4.07	Corraberra sandstone: brown and grey silicified fine to medium sandstone		0	M	T
16	24-25	1231	4.30	Shale: Pale grey and brown interbedded shale and sil. fine sandstone	Trace sulfides, mica	0	CD	CD
16	46-47	1107	3.15	Corraberra sandstone: banded maroon and greenish grey silicified fine sandstone / quartzite with purple micaceous mudstone interbeds.		0	M	T
14	13-14	959	2.15	Pale Pistachio plastic clay		0	M	M
16	10-11	854	2.67	Banded quartzite and pale grey to white clays		T	M	SD
16	37-38	789	2.45	Shale: Reddish brown laminated shale	Trace sulfides	0	M	T
16	30-31	747	2.14	Arcoona quartzite, pale greenish grey, some micaceous bands	Trace sulfides	0	M	M
14	23-24	690	2.90	Greenish grey clay		0	M	T
14	19-20	671	1.47	Pale olive grey clay		0	M	M
16	1-2	647	16.7	Reddish brown plastic sandy clay	Minor calcrete	M	0	T
12	9-10	633	1.80	Greyish yellow clay bands in grey silicified sandstone quartzite		0	T	T
14	40-41	628	1.39	Corraberra sandstone : maroon and grey silicified fine to med. sandstone	Minor bluish grey fine sandstone bands	0	T	T

13	10-11	586	1.19	Pale greenish grey clay	Minor quartzite bands	0	T	T
13	21-22	545	1.49	Pale grey clay		0	T	T
13	7-8	513	2.14	Pale greenish grey to white clay	Minor quartzite bands	0	T	T
12	1–2	512	23.3	Reddish brown plastic sandy clay	Minor calcrete nodules	M	0	T
14	55-56	466	1.62	Corraberra sandstone: Maroon silicified fine to med. Sandstone (below water table)	Minor blueish grey siltstone bands	0	T	0
13	31-32	449	1.71	Corraberra sandstone maroon silicified medium sandstone	Minor grey fine sandstone	0	T	T
16	77-78	447	1.23	Corraberra sandstone: Grey and purple silicified fine to med. sandstone (below water table)	Minor brown micaceous siltstone bands	0	T	0
41	31-32	386	3.69	Micaceous sandstone: Highly micaceous, pinkish-grey purple fine to medium sandstone	Trace yellowish grey clay bands	T	T	T
16	2-3	239	5.34	Silcrete; pale grey		M	0	0
10	23-24	182	0.42	Arcoona quartzite: pale grey		0	T	T
7	9-10	154	1.53	Arcoona quartzite: Pale grey	Minor white clay bands	0	0	T

Figures 1. Mass fraction of water [g/g] graphed as a function of solid material distance divided by the square root of time for experiments terminated after different times as identified on the graphs. The material length is the cumulative mass of soil, per unit area of cross section of column, measured away from the water source.

a) Sample 16:1-2m

b) Sample 16:10-11m, and

c) Sample 14:19-20m.

These figures illustrate similarity of water profiles measured at different times when expressed as distance divided by the square root of time.

Figure 1a
Water content profiles
Sample#16:1-2

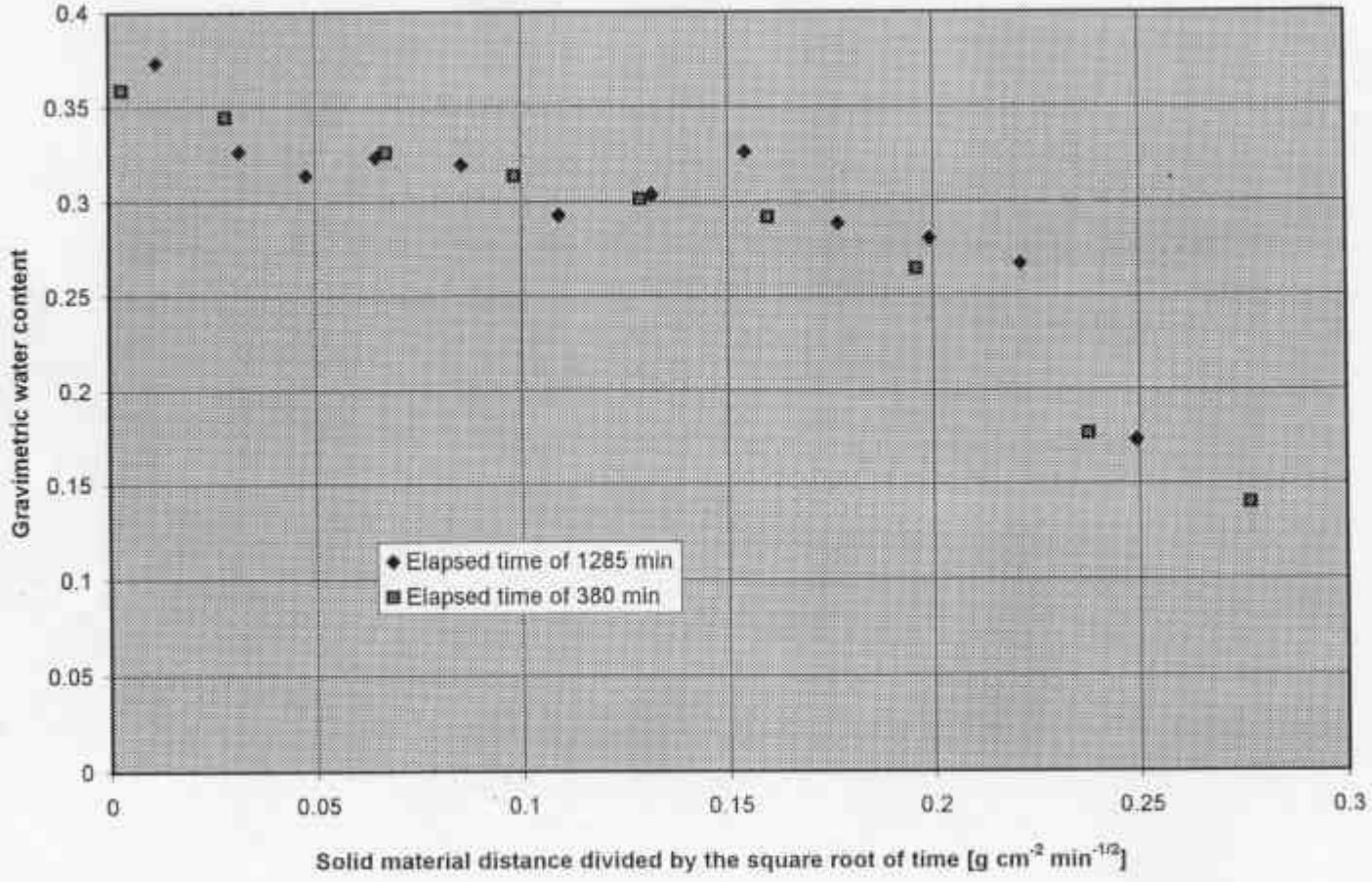

Figure 1b
Water content profiles
Sample #16:10-11m

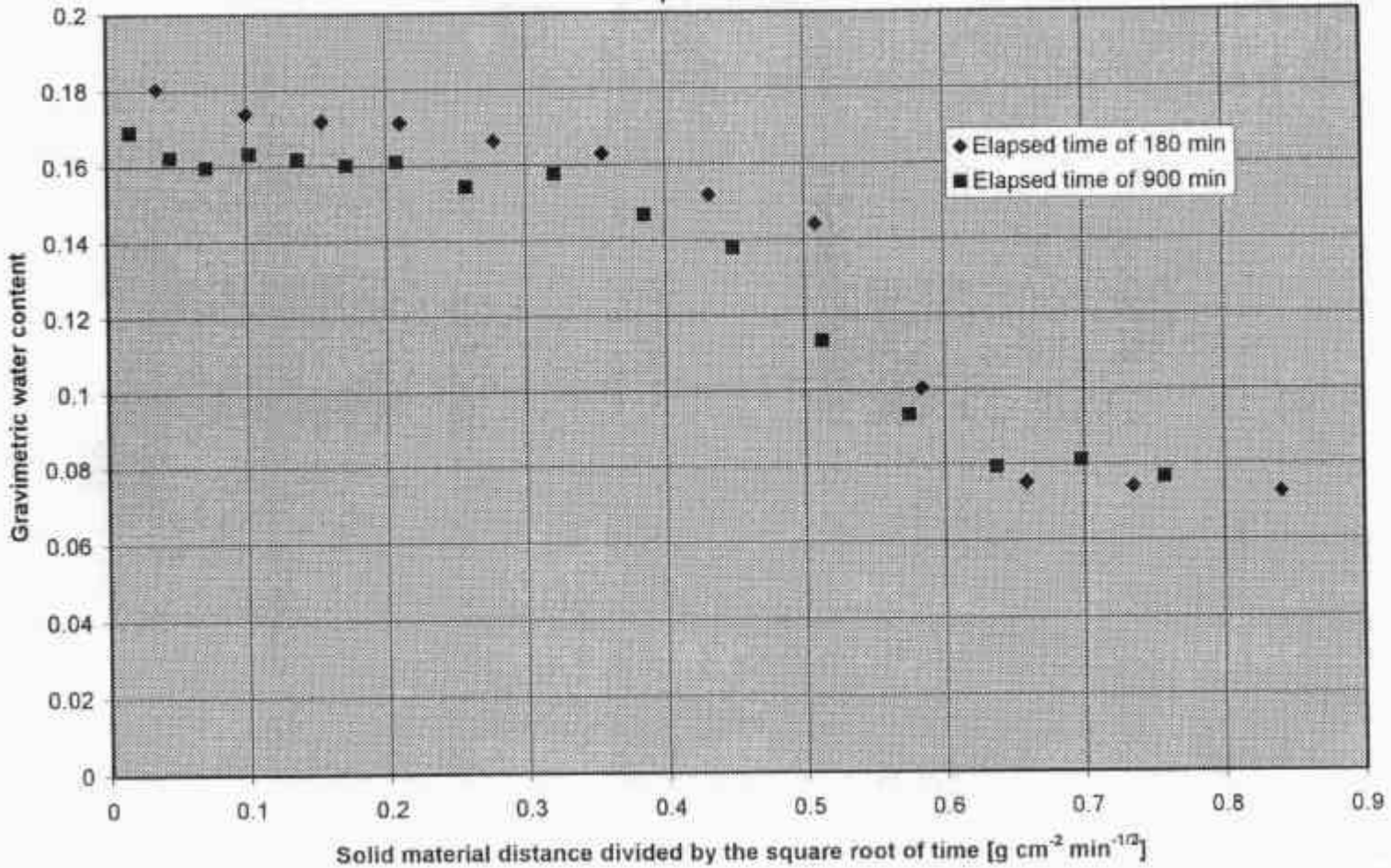

Figure 1c
Water content profiles
Sample #14:19-20

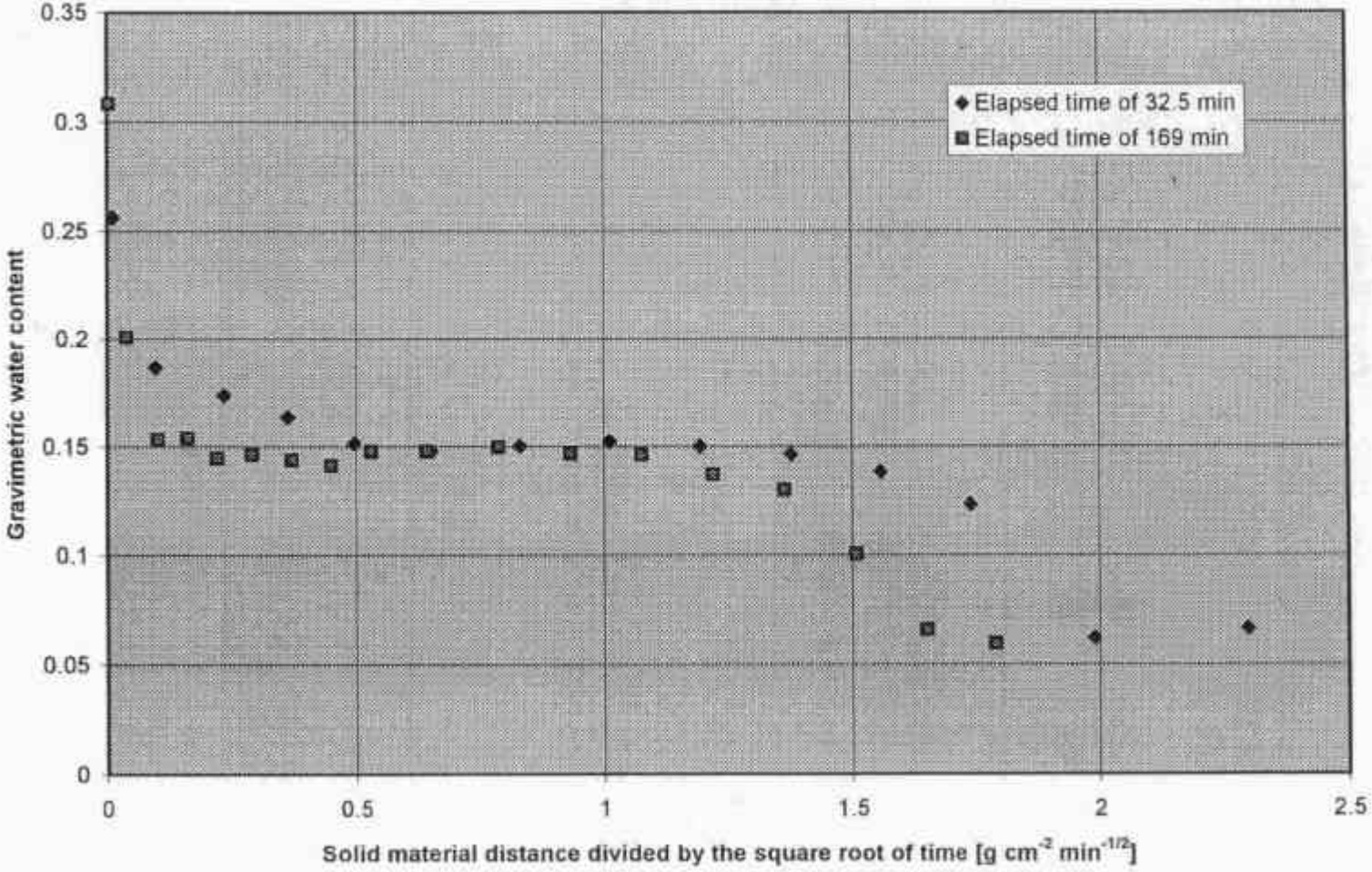

Figures 2. Normalised soil solution concentrations of water soluble salts and tritiated water graphed as a function of solid material distance divided by the square root of time. Symbols for the solutes and tritium for experiments terminated after different times are identified on the graphs. Tritium concentrations are normalised relative to the tritium concentration in the inflowing solution (479 Bq/mL). The soluble salt concentrations are expressed in conductivity units of mS/cm and normalised with regard to the measured values at the distal ends of the columns.

a) Sample 16:1-2m. The normalising conductivity is 200 mS/cm,

b) Sample 16:10-11m. The normalising conductivity is 200 mS/cm,

c) Sample 14:19-20m. The normalising conductivity is 100 mS/cm.

These figures illustrate similarity of tritium and soluble salt profiles measured at different times when expressed as distance divided by the square root of time. They also show how the infiltrating water, characterised by the presence of tritium, appears to displace the water originally present (characterised by the high concentration of salts). In this sense, tritium moves with the water and is indistinguishable from it.

Figure 2a
Tritium and soluble salt profiles
Sample #16:1-2

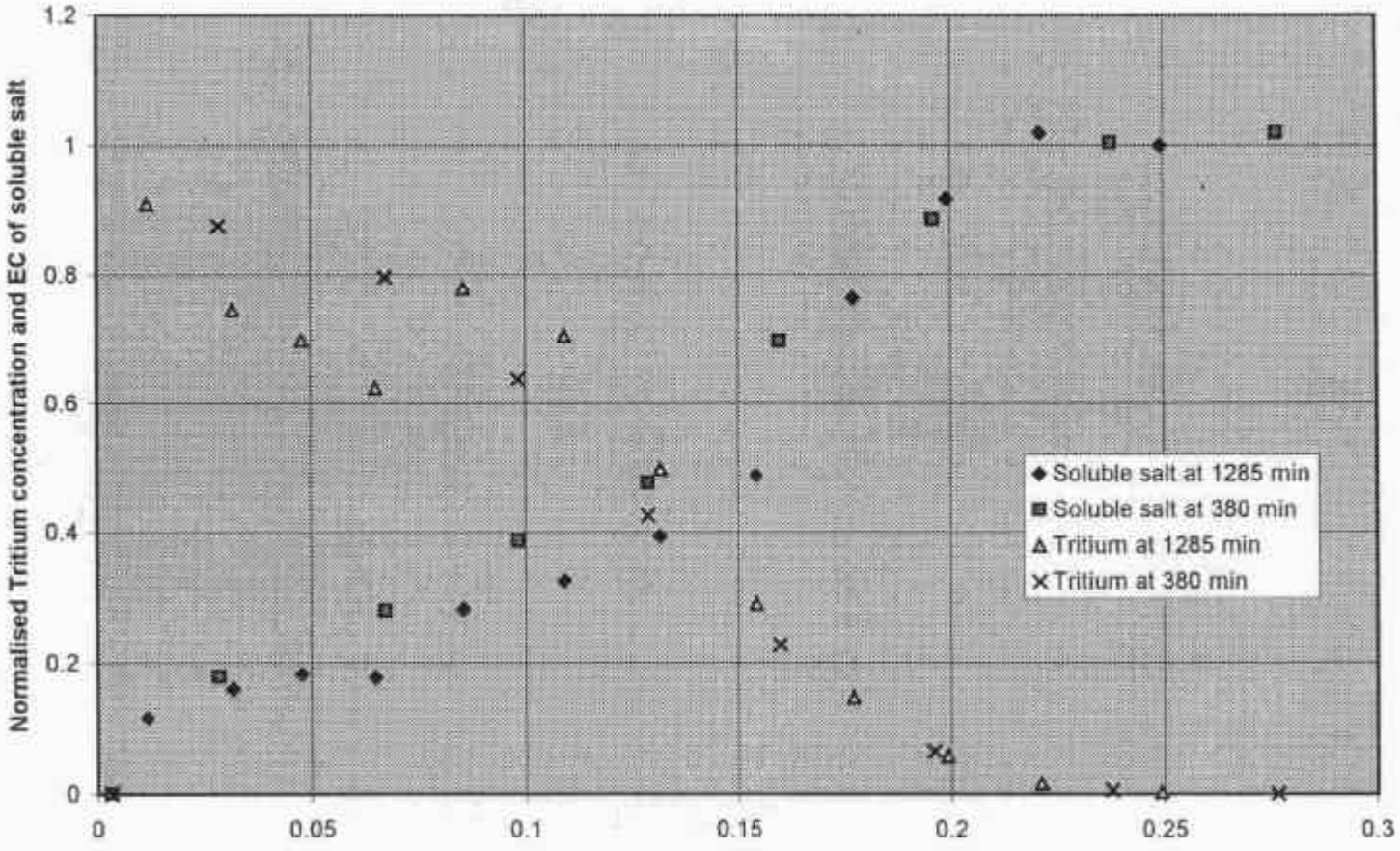

Figure 2b
Tritium and soluble salt profiles
Sample #16:10-11

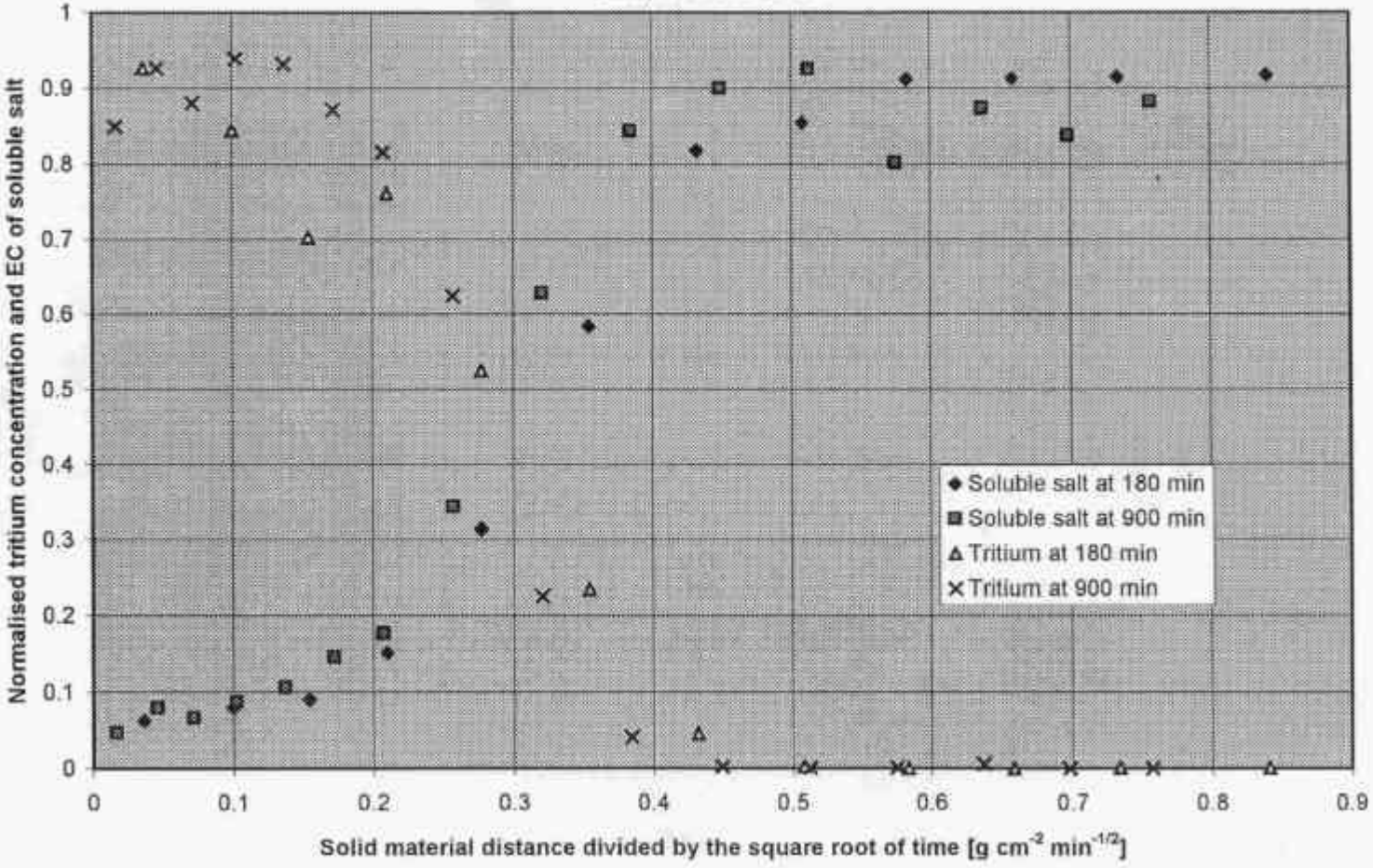

Figure 2c
Tritium and soluble salt profiles
Sample #14:19-20

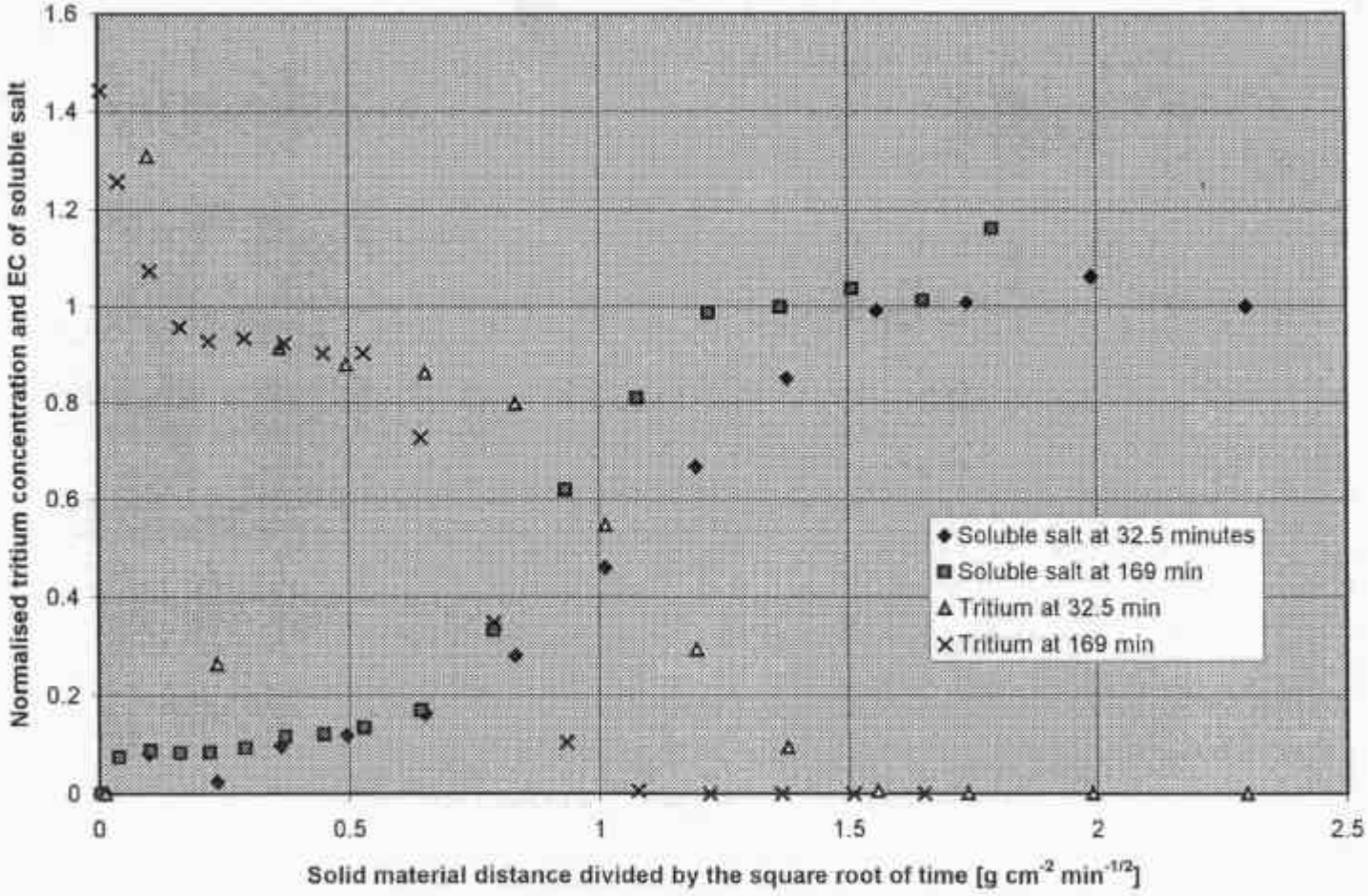

Figures 3. Normalised soil solution concentrations of water soluble salts and tritiated water graphed as a function of a water based material coordinate divided by the square root of time. Symbols for the solutes and tritium for experiments terminated after different times are identified on the graphs. Tritium concentrations are normalized relative to the tritium concentration in the inflowing solution (479 Bq/mL). The soluble salt concentrations are expressed in conductivity units of mS/cm and normalised with regard to the measured values at the distal ends of the columns.

a) Sample 16:1-2. The normalising conductivity is 200 mS/cm,

b) Sample 16:10-11. The normalising conductivity is 200 mS/cm,

c) Sample 14:19-20. The normalising conductivity is 100 mS/cm.

These figures illustrate similarity of tritium and soluble salt profiles measured at different times when expressed as distance, defined by the water distribution in the soil, divided by the square root of time. The origin of this coordinate system is the "piston front" which would exist if the infiltrating water displaced in its entirety, the water originally present in the soil. The data of Fig.3c, in particular, show that the scatter in data in Fig. 2c arises because of uneven packing in the column of Samples 14:19-20 and not from unexpected physico-chemical effects.

Figure 3a
Tritium and soluble salts profiles
Sample #16:1-2

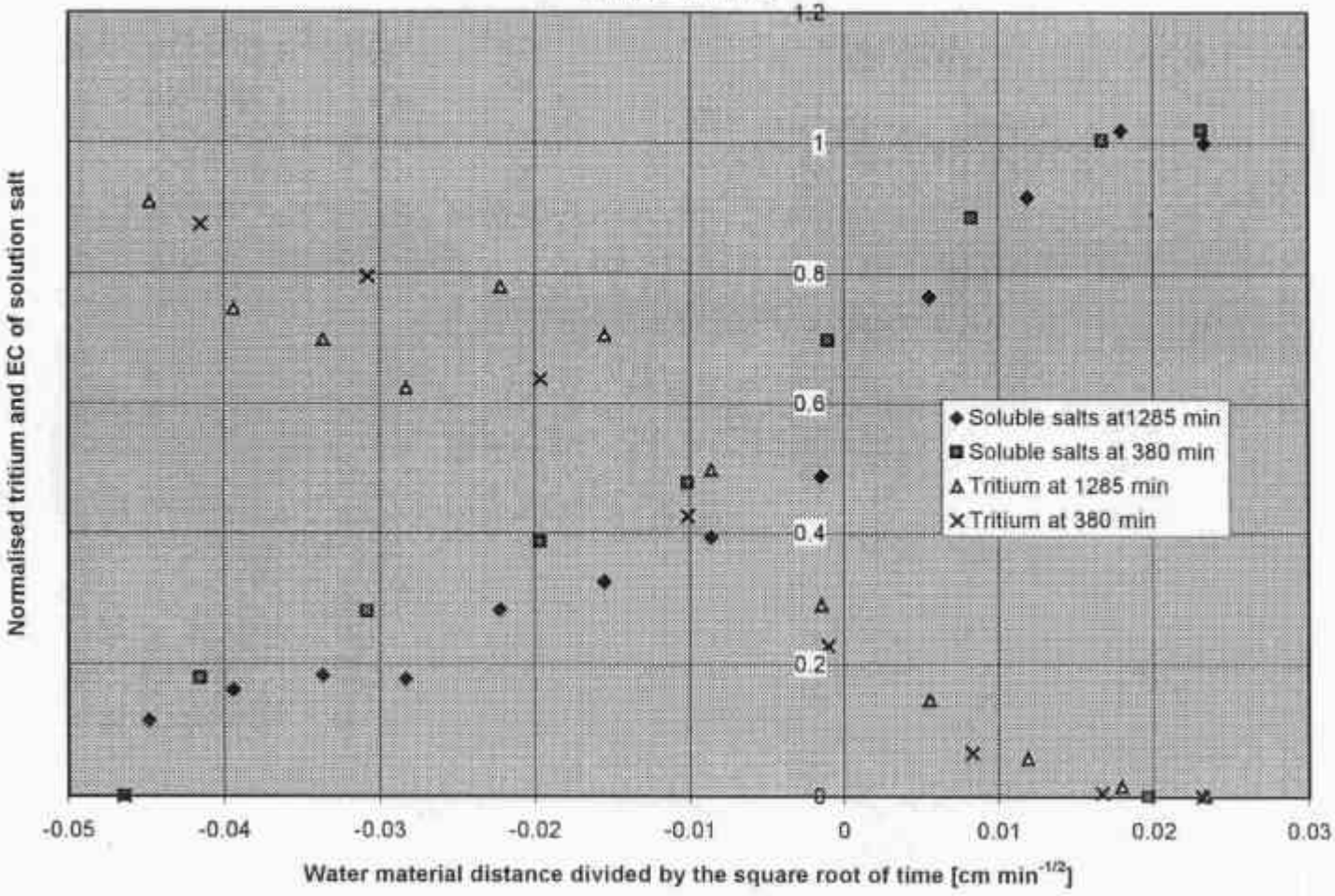

Figure 3b
Tritium and soluble salts profiles
Sample #16:10-11

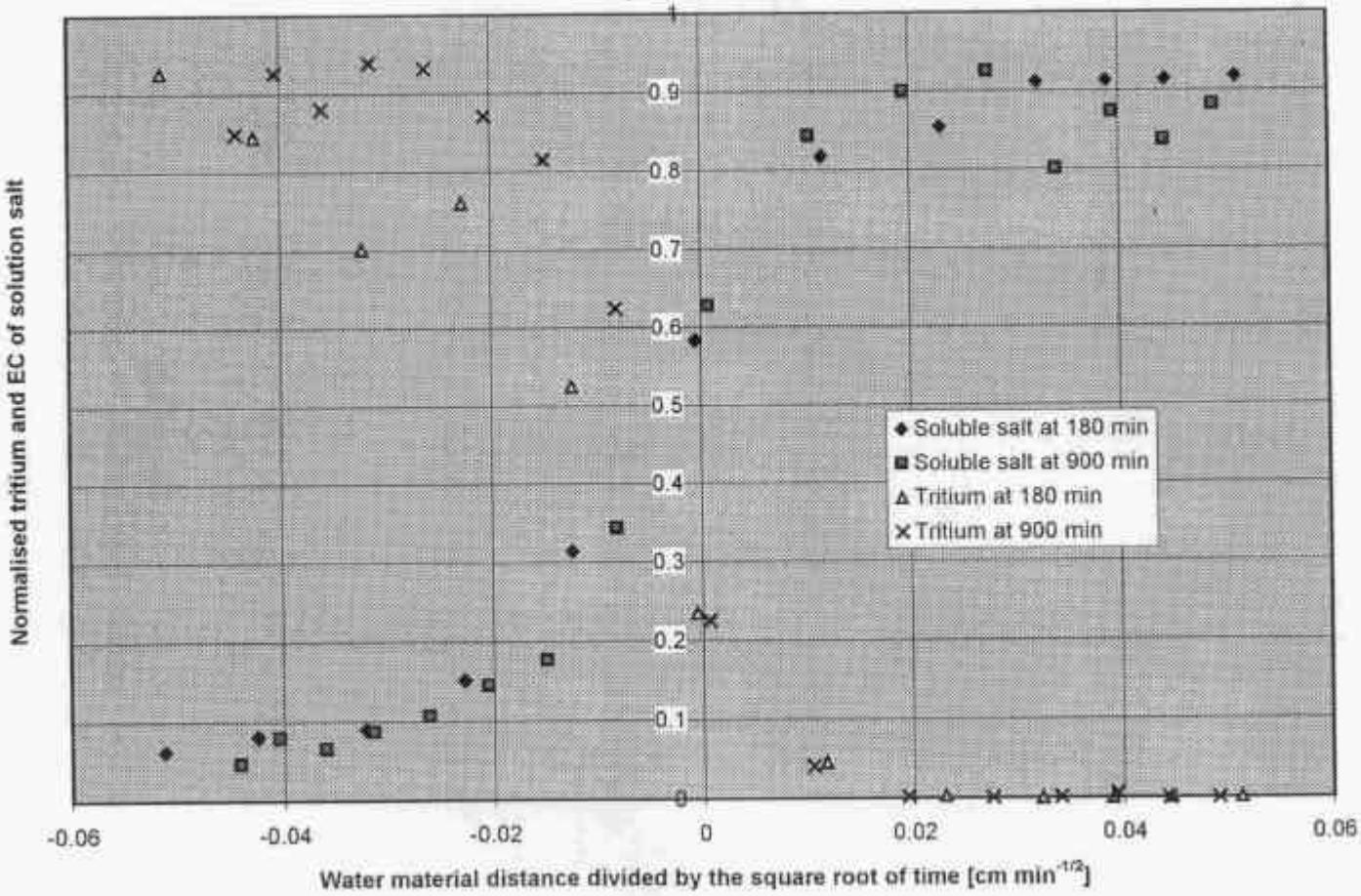

Figure 3c
Tritium and water soluble salt profiles
Sample #14:19-20

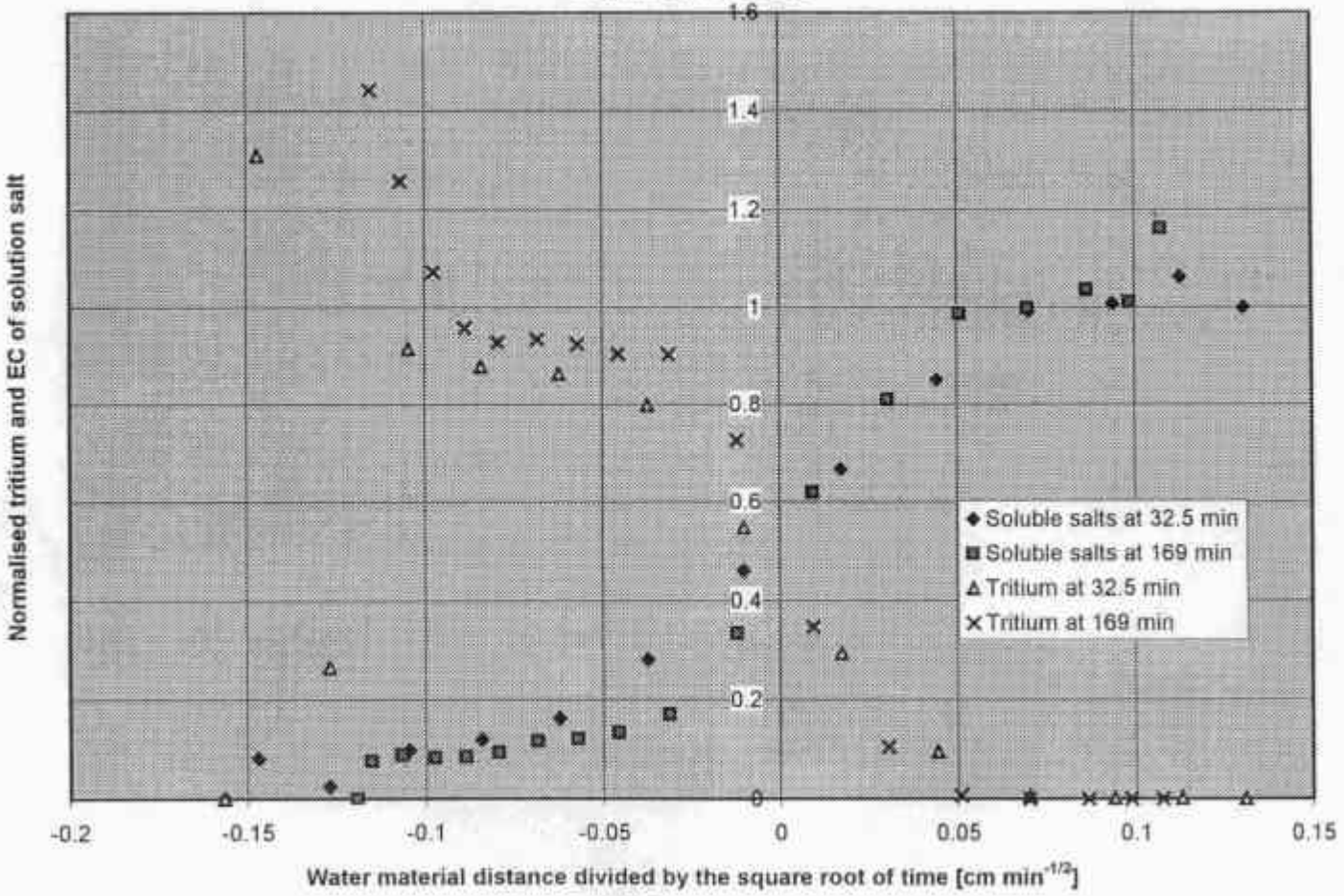

Figures 4. The distribution of ^{60}Co and ^{137}Cs in columns of soil. These data are graphed as a function of solid based material coordinate divided by the square root of time. Symbols for these nuclides, for experiments terminated after different times, are identified on the graphs.

a) Sample 16:1-2m.

b) Sample 16:10-11m, and

c) Sample 14:19-20m.

It is important to note that, in Fig. 4a and 4b, the nuclides were retained in the first section of the column only and the impression of a "profile of nuclide" is illusory. Fig. 4c, on the other hand shows that ^{60}Co had moved significant distances along the columns with the emergence of a well-defined concentration profile.

Figure 4a
Cobalt and cesium profiles
Sample #16:1-2

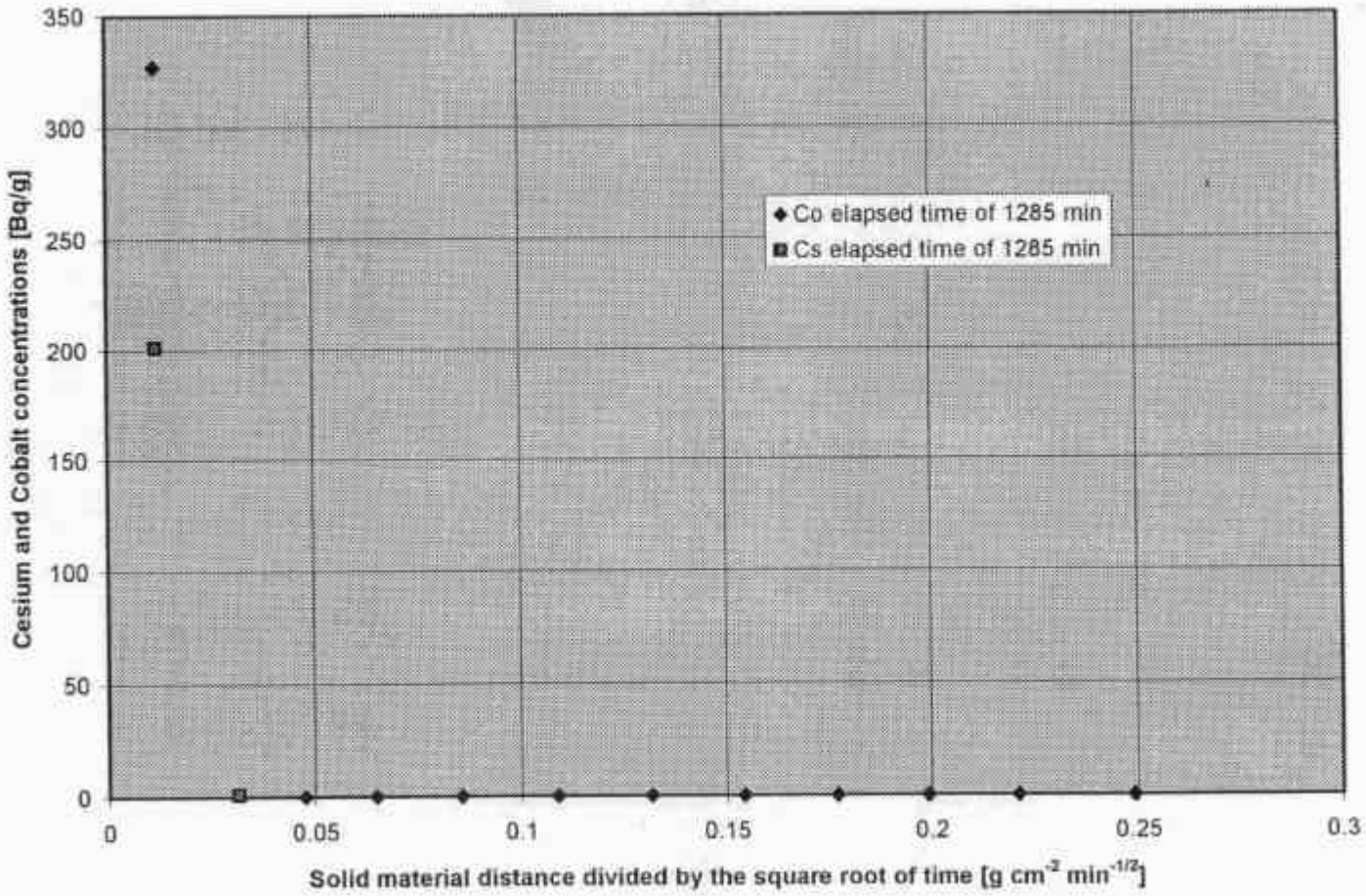

Figure 4b
Cobalt and Cesium profiles
Sample #16:10-11

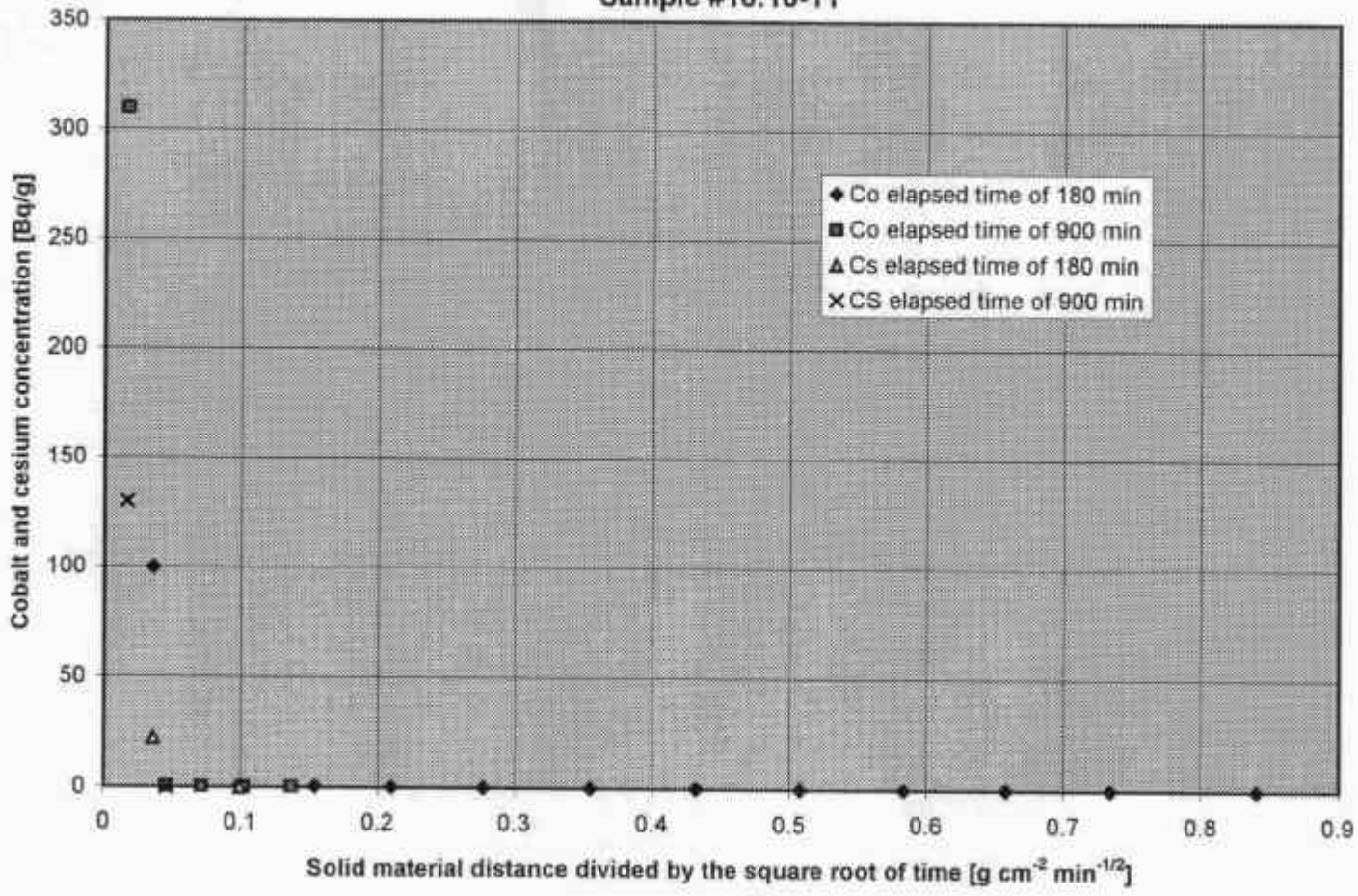

Figure 4c
Cobalt and cesium profiles
Sample #14:19-20